AN EXPLORATORY ANALYSIS OF *IN SITU* HYPERSPECTRAL DATA FOR BROADLEAF SPECIES RECOGNITION

R. Pu

Department of Geography, University of South Florida, 4202 E. Fowler Ave., NES 107, Tampa, FL 33620 USA - rpu@cas.usf.edu

Commission VII, WG VII/3

ABSTRACT:

Timely and accurate identification of tree species by spectral methods is crucial for forest and urban ecological management. It has been proved that traditional methods and data cannot meet such requirements. In this study, a total of 394 reflectance spectra (between 350 and 2500 nm) from foliage branches or canopy of 11 important urban forest broadleaf species were measured in the City of Tampa, Florida, U.S. with a spectrometer. The 11 species include American Elm (*Ulmus americana*), Bluejack Oak (*Q. incana*), Crape Myrtle (*Lagerstroemia indica*), Laurel Oak (*Q. laurifolia*), Live Oak (*Q. virginiana*), Southern Magnolia (*Magnolia grandiflora*), Persimmon (*Diospyros virginiana*), Red Maple (*Acer rubrum*), Sand Live Oak (*Q. geminata*), American Sycamore (*Platanus occidentalis*), and Turkey Oak (*Q. laevis*). A total of 46 spectral variables, including normalized spectra, derivative spectra, spectral vegetation indices, spectral position variables, and spectral absorption features were extracted and analyzed from the *in situ* hyperspectral measurements. Two classification algorithms were used to identify the 11 broadleaf species: a non-linear artificial neural network (ANN) and a linear discriminant analysis (LDA). An ANOVA analysis indicates that the 30 selected spectral variables are effective to differentiate the 11 species. The 30 selected spectral variables account for water absorption features at 970 nm, 1200, and 1750 nm and reflect characteristics of pigments in tree leaves, especially variability of chlorophyll content in leaves. The experimental results indicate that both classification algorithms (ANN and LDA) have produced acceptable accuracies (OAA from 86.3 % to 87.8%, Kappa from 0.83 to 0.87) and have a similar performance for classifying the 11 broadleaf species with input of the 30 selected spectral variables. The preliminary results of identifying the 11 species with the *in situ* hyperspectral data imply that current remote-sensing techniques are still difficult but possible to identify similar species to such 11 broadleaf species with an acceptable accuracy.

1. INTRODUCTION

The need for detailed forest parameters (species, size, and number of trees), biophysical properties (canopy density and leaf area index (LAI)), and canopy chemical composition over large land holdings in the U.S., has increased markedly in the last decade (Gong et al., 1999). Mapping forest area or tree species identification is usually based on aerial photo interpretation and moderate-resolution satellite image classification. Aerial photo interpretation is dependent on the experience of photo interpreters and some experiments indicate large discrepancies among photo interpretation by different interpreters (Biging et al., 1991; Gong and Chen, 1992). It is also difficult to develop detailed accurate individual tree crowns and tree canopy maps because of the limited spatial resolution of existing satellite imagery such as SPOT HRV, and Landsat TM/ETM+ data (Congalton et al., 1991; Brockhaus and Khorram, 1992; Franklin, 1994; Carreiras et al., 2006).

During the last two decades, researchers have used high spatial resolution satellite sensors (< 5 m resolution, such as IKONOS and QuickBird) and hyperspectral data [such as Airborne Visible Infrared Imaging Spectrometer (AVIRIS)] to extract detailed forest parameters such as tree species and mapping forest canopy (e.g., Wang et al., 2004; Xiao et al., 2004; Buddenbaum et al., 2005; Johansen and Phinn, 2006). The preliminarily results of evaluating capabilities of those high resolution data in identifying tree species and mapping tree canopy indicate that the accuracy is not desirable (Asner et al., 2002; Carleer and Wolff, 2004; Johansen and Phinn, 2006). In

mapping urban forest species with hyperspectral image data AVIRIS, Xiao et al. (2004) reported a relatively low overall accuracy (OAA=70%) for identifying 16 tree species with AVIRIS data although they successfully discriminated between three forest types with OAA=94%. Classifying coniferous tree species with HyMap using geostatistical methods, the classification of accuracy (Kappa) of the tree species was only 0.74, a result comparable to that obtained with stem density information derived from high spatial resolution imagery (Buddenbaum et al., 2005). Therefore, it is still necessary to conduct further research in recognizing tree species and mapping tree canopy using either high spatial or high spectral resolution remote-sensing data, including *in situ* hyperspectral measurements (e.g., Gong et al., 1997; Cochrane, 2000).

In this study, further evaluation of the capabilities of *in situ* hyperspectral data in recognizing 11 broadleaf species in an urban environment was conducted with *in situ* hyperspectral measurements, collected with an ASD spectrometer (FieldSpec®3, Analytical Spectral Devices, Inc., U.S.). Therefore, the objectives of this analysis consist of (1) examining the analysis capability of hyperspectral data for identifying major broadleaf tree species in the City of Tampa, Florida, (2) evaluating effectiveness of spectral features extracted from the *in situ* hyperspectral data, and (3) comparing the performance of the artificial neural network (ANN) and linear discriminant analysis (LDA) techniques in identifying broadleaf species.

2. STUDY SITE AND HYPERSPECTRAL DATA COLLECTION

2.1 Study Site

The City of Tampa was selected as study area. It is the largest city on the west coast of Florida consisting of approximately 285 sq. km. The population is increasing and is currently estimated at approximately 335,000 people (www.tampagov.net accessed on Nov. 26, 2007). The city is located at approximately 28° N and 82° W (Figure 1). Historically, the natural plant communities of the Tampa Bay region included pine flatwoods, cypress domes, hardwood hammocks, high pine forests, freshwater marshes, and mangrove forests. Based on the City of Tampa Urban Ecological Analysis (Campbell and Landry, 1999), important, dominant urban tree species include American Elm (*Ulmus americana*), Bluejack Oak (*Q. incana*), Crape Myrtle (*Lagerstroemia indica*), Laurel Oak (*Q. laurifolia*), Live Oak (*Q. virginiana*), Southern Magnolia (*Magnolia grandiflora*), Persimmon (*Diospyros virginiana*), Red Maple (*Acer rubrum*), Sand Live Oak (*Q. geminata*), American Sycamore (*Platanus occidentalis*), Turkey Oak (*Q. laevis*), Slash Pine (*Pinus elliottii*), and Longleaf Pine (*Pinus palustris*). Other dominant tree species within the City of Tampa include Cabbage Palm (*Sabal palmetto*), Queen Palm (*Syagrus romanzoffiana*), Citrus (*Citrus spp.*), Goldenrain Tree (*Koelreuteria paniculata*), Bottlebrush (*Callistemon viminale*), and Water Oak (*Q. nigra*), etc. In this analysis, a total of 11 broadleaf species (Table 1) were selected for testing the capability of *in situ* hyperspectral data for discriminating between species. Note that shorthand abbreviations for tree species discussed throughout this paper can be found in Table 1 in parentheses after the common name of the tree species.
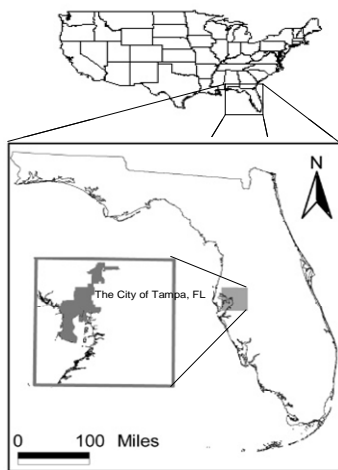
Figure 1. A location map of the study area

2.2 *In Situ* Hyperspectral Data Collection

A full-range Analytical Spectral Device (ASD) (FieldSpec®3, Analytical Spectral Devices, Inc., U.S.) was used to collect spectral reflectance measurements from the 11 broadleaf tree species in the city area, which are a subset of urban forest species within the Tampa Bay area. The ASD instrument consists of three separate spectrometers and covers a spectral range of 350 nm to 2500 nm.

Tree species	Number of trees	Train samples	Test samples	Total
American Elm (Elm)	25	22	12	34
Bluejack Oak (Blue)	20	17	8	25
Crape Myrtle (Crap)	20	27	13	40
Laurel Oak (Laur)	31	24	13	37
Live Oak (Live)	26	24	11	35
Southern Magnolia (Magn)	20	30	16	46
Persimmon (Pers)	29	22	11	33
Red Maple (Mapl)	27	24	12	36
Sand Live Oak (Sand)	23	25	12	37
American Sycamore (Syca)	16	25	12	37
Turkey Oak (Turk)	28	22	12	34
Total	**265**	**262**	**132**	**394**

Table 1. Spectral measurements taken from 11 broadleaf species.

In the field, at least 20 trees of each species (except Syca) were measured to account for spectral variation and spatial distribution. The spectral measurements were collected from top, middle and low foliage branches from the crowns of individual species. Tree heights lower than 7 m for most sampled trees were generally selected because of the logistical difficulties with measuring spectra from the top of tall trees. A ladder with an effective height of 5 m was used for collecting spectral measurements. To ensure that relatively pure spectra from individual trees of difference species were collected, the data acquisition was executed with a careful selection of view area from tree foliage branches to avoid or lessen the effect of background on target spectra. 0ne to three spectra were collected from individual trees. Because of the difficulty in separating a shadow/shaded area from a sunlit area from a tree crown, only fully sunlit areas were measured. Each spectral measurement was repeated ten times to obtain reliable mean and variance estimates. In this manner, a total of 394 spectral measurements were collected from the different foliage branches of the 11 broadleaf species in the City of Tampa (Table 1).

3. ANALYSIS METHODS

3.1 Preprocessing of Spectral Measurements

The following preprocessing of spectral measurement was performed. First, spectral curves were truncated below 400 nm and above 2400 nm because the measurements were extremely noisy outside of this range. Approximately 2000 bands remain, each with a width of about 1 nm. Next, curve smoothing was used with a simple average over blocks of five neighboring bands. The spectral curves for constant area were then normalized by dividing the mean reflectance for that curve. That is, a spectral reflectance curve ρ_i was replaced with $\rho_i / (\frac{1}{k} \sum_{i=1}^{k} \rho_i)$, where, k represents the total bands of the spectral reflectance. The benefit of such normalization is the suppression of illumination differences. Figure 2(a) shows a plot of unnormalized curves versus band wavelength for two observations of each of the five oak species (Blue, Laur, Live, Sand and Turk). Figure 2(b) shows the same curves of Figure 2(a) after normalization. Notice that the clearer separation between the species over a wide range of wavelength in Figure 2(b). Figure 2(c) shows a plot of normalized curves versus band wavelength for all the 11 species (Elm through Turk).

3.2 Extraction of Spectral Variables

Forty-six spectral variables (Table 2), including normalized spectra, derivative spectra, spectral vegetation indices, spectral

position variables, and spectral absorption features were extracted from the *in situ* hyperspectral measurements and analyzed for classifying the 11 species.
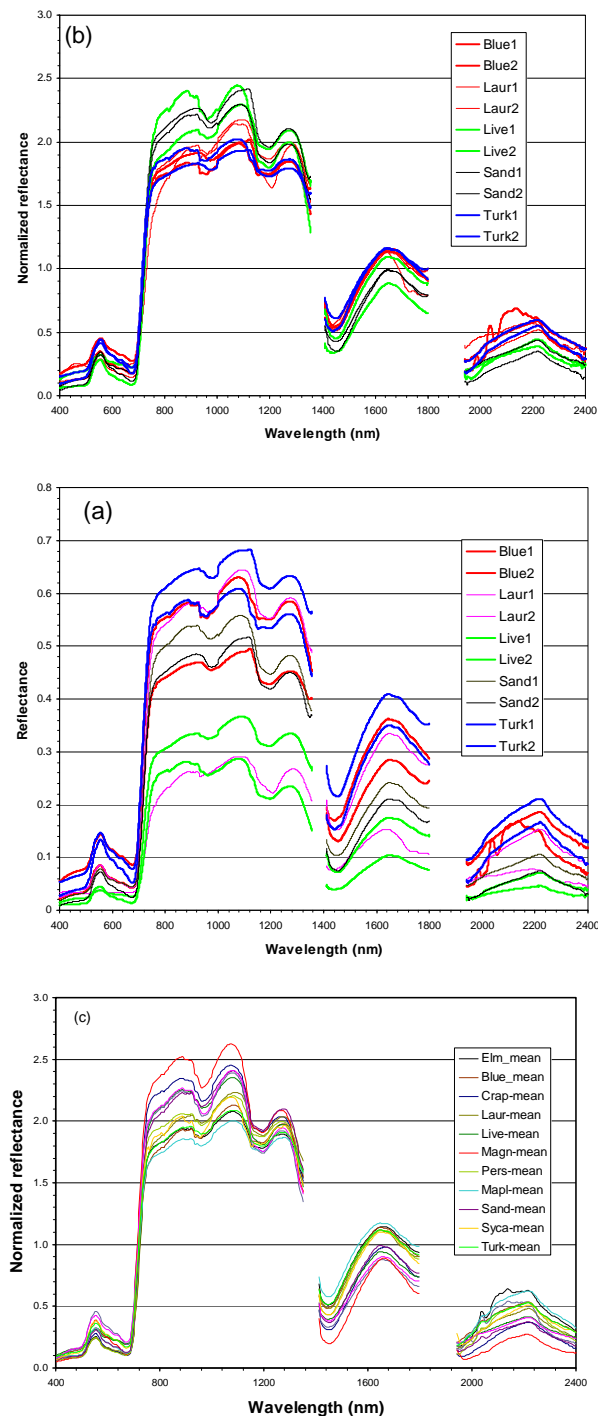
Figure 2. Figure 2(a) shows a plot of unnormalized curves of five oak species versus band wavelength for two observations of each of the five oak species (Blue, Laur, Live, Sand and Turk). Figure 2(b) shows the same curves of Figure 2(a) after normalization. Figure 2(c) shows a plot of normalized curves versus band wavelength for all the 11 species (Elm through Turk).

3.3 ANOVA

To select a subset of spectral variables from the total 46 spectral variables for running ANN and LAD for species recognition, an one-way ANOVA analysis was performed. This was done based on greater spectral separability between any two species (paired-species) of the 11 species, using the SPSS statistical package (www.spss.com, 2007). For any paired-species from the 11 species, all spectral measurements for the paired-species were used to conduct the ANOVA analysis across the 46 spectral variables (Table 2). Then based on the degree of spectral separability of each spectral variable between the paired-species, a statistical frequency was calculated at probability levels $p \leq 0.01$ and $p \leq 0.05$ for each spectral variable. For this analysis, a maximum frequency at either $p \leq 0.01$ or $p \leq 0.05$ is 55 (because of $_{11}C_2 = 55$).

3.4 Species Recognition Schemes

Two supervised classification schemes were employed for the broadleaf tree classification: non-linear artificial neural network (ANN) and linear discriminant analysis (LDA). In this analysis, a feed-forward ANN algorithm was used for classifying the 11 species. An LDA classifier was also used to classify the 11 tree species with inputs of the same subset of spectral variables as for ANN to compare with the classified results by ANN. The procedure DISCRIM in the SAS system (SAS Institute, 1991) was used.

Two sets of samples were allocated - training and test samples, from a total of 394 samples collected from 11 tree species. The training samples were used for training ANN and LDA while test samples are used to evaluate the tree species recognition accuracies, generated with ANN and LDA. About 2/3 of the samples were used for training and about 1/3 of the samples were used as test samples. This procedure was repeated three times (runs) (see Table 1) to obtain three different sets of test samples (but training sets with a part overlaid between any two sets). Finally, an overall accuracy (OAA) and Kappa index are calculated from a confusion matrix produced with the test samples using ANN and LDA.

4. RESULTS AND ANALYSIS

4.1 ANOVA

After the *in situ* hyperspectral data were preprocessed, including smoothing and normalization, according to the definitions for spectral variables listed in Table 2, the 46 spectral variables were extracted. An one-way ANOVA analysis was first performed for all the extracted spectral variables from which a subset of spectral variables was selected. If the frequency threshold was set to greater than the half of maximum possible frequency of 55, a total of 30 spectral variables were selected.

Among the 30 selected spectral variables, all 10 VIs are included, which imply that those VIs make a substantial contribution to separating most of the 11 tree species. The 30 selected spectral variables can be further classified into two groups. The first group of spectral variables mainly describes the variation of foliage water content among the difference species and its spectral variables consist of WI, DSWI, Ratio1200, E-1D, NDWI, DEP-975, AREA-975, H-WP, PRI, DEP-1200, AREA-1200, Ratio975, and WID-1200. The

Spectral variables	Characteristic of the plant related with the variable/index	Definition	Described by
A-1D, B-1D, C-1D, D-1D, E-1D, F-1D, G-1D, H-1D, I-1D, J-1D, maximum 1st derivative spectra	Pigments absorption in visible region and water, cellulose, starch and lignin absorption in NIR and SWIR.	Maximum 1st derivative spectra of 10 'slopes' : blue edge , yellow edge and red edge and other 7 'slopesi in NIR and SWIR regions	Gong et al., 2002 Pu et al., 2004
A-WP, B-WP, C-WP, D-WP, E-WP, F-WP, G-WP, H-WP, I-WP, J-WP, spectral position variables corresponding "1Ds"	Pigments absorption in visible region and water, cellulose, starch and lignin absorption in NIR and SWIR.	Corresponding spectral positions of "1Ds" of 10 'slopes' : blue edge , yellow edge and red edge and other 7 'slopesi in NIR and SWIR regions	Gong et al., 2002 Pu et al., 2004
R550	Chlorophyll content	Reflectance at 550 nm	Thomas and Gausman, 1977
R680	Chlorophyll content	Reflectance at 680 nm	Thomas and Gausman, 1977
WI, Water Index	Water status	R_{900}/R_{970}	Peñuelas et al., 1997
NDVI, Normalized Difference Vegetation Index	Photosynthetic area; cell structure multi-reflected spectra	$(R_{NIR}-R_R)/(R_{NIR}+R_R)$	Rouse et al., 1973
SR, Simple Ratio	Same as **NDVI**	R_{NIR}/R_R	Jordan, 1969
PRI, Photochemical Reflectance Index	Water stress	$(R_{531}-R_{570})/(R_{531}+R_{570})$	Thenot et al., 2002
SIPI, Structural Independent Pigment Index	Carotenoids: chlorophyll a ratio	$(R_{445}-R_{800})/(R_{680}-R_{800})$	Peñuelas and Filella, 1998
NPCI, Normalized total Pigment to Chlorophyll Index	Senescence	$(R_{680}-R_{430})/(R_{680}+R_{430})$	Peñuelas et al., 1994
NPQI, Normalized Phaeophytinization Index	Senescence	$(R_{415}-R_{435})/(R_{435}+R_{435})$	Barnes et al., 1992 Peñuelas et al., 1995
LCI, Leaf Chlorophyll Index	Chlorophyll content	$(R_{850}-R_{710})/(R_{850}+R_{680})$	Datt , 1999
NDWI, ND Water Index	Water status	$(R_{860}-R_{1240})/(R_{860}+R_{1240})$	Datt et al., 2003 Gao, 1996
DSWI, Disease water stress index	Water status	$(R_{802}+R_{547})/(R_{1657}+R_{682})$	Galvão et al., 2005
RATIO₉₇₅ 3-band ratio at 975 nm	Water status	$2*R_{960-990}/(R_{920-940}+ R_{1090-1110})$	Pu et al., 2003
RATIO₁₂₀₀ 3-band ratio at 1200 nm	Water status	$2*R_{1180-1220}/(R_{1090-1110}+ R_{1265-1285})$	Pu et al., 2003
WP-975: wavelength position at 975 nm	Water absorption feature at 975 nm	See reference for the defiinition of wavelength position at 975 nm	Pu et al., 2003
DEP-975 absorption depth at 975 nm	Water absorption feature at 975 nm	See reference for the defiinition of absorption depth at 975 nm	Pu et al., 2003
WID-975 absorption width at 975 nm	Water absorption feature at 975 nm	See reference for the defiinition of absorption width at 975 nm	Pu et al., 2003
AREA-975 absorption area at 975 nm	Water absorption feature at 975 nm	See reference for the defiinition of absorption area at 975 nm	Pu et al., 2003
WP-1200: wavelength position at 1200 nm	Water absorption feature at 1200 nm	See reference for the defiinition of wavelength position at 1200 nm	Pu et al., 2003
DEP-1200 absorption depth at 1200 nm	Water absorption feature at 1200 nm	See reference for the defiinition of absorption depth at 1200 nm	Pu et al., 2003
WID-1200 absorption width at 1200 nm	Water absorption feature at 1200 nm	See reference for the defiinition of absorption width at 1200 nm	Pu et al., 2003
AREA-1200 absorption area at 1200 nm	Water absorption feature at 1200 nm	See reference for the defiinition of absorption area at 1200 nm	Pu et al., 2003
WP-1750: wavelength position at 1750 nm	Water absorption feature at 1750 nm	See reference for the defiinition of wavelength position at 1750 nm	Tian et al., 2001 Pu et al., 2003
DEP-1750 absorption depth at 1750 nm	Water absorption feature at 1750 nm	See reference for the defiinition of absorption depth at 1750 nm	Tian et al., 2001 Pu et al., 2003
WID-1750 absorption width at 1750 nm	Water absorption feature at 1750 nm	See reference for the defiinition of absorption width at 1750 nm	Tian et al., 2001 Pu et al., 2003
AREA-1750 absorption area at 1750 nm	Water absorption feature at 1750 nm	See reference for the defiinition of absorption area at 1750 nm	Tian et al., 2001 Pu et al., 2003

Table 2. Summary of 46 spectral variables extracted from the *in situ* hyperspectral measurements for this analysis.

second group of spectral variables relates the characteristics and pigment status (primarily chlorophyll) of leaves among the difference species and its spectral variables consist of C-1D, A-1D, B-1D, R550, A-WP, SIPI, NPQI, LCI, B-WP, SR, J-1D, NPCI C-WP, R680, H-1D, and F-1D.

4.2 Species Recognition

To train and test the three-layer ANN structure for classifying the 11 species (including five oak species), the input of 30 selected spectral variables was first normalized to the range of [0, 1]. The output layer had 11 nodes corresponding 11 species (or 5 nodes for 5 oak species). To find a better ANN structure, various combinations of learning rate (η), momentum

coefficient (α) and number of nodes in a hidden layer (h1) were tested using the first training/test data set (Table 1). In considering relatively small variation of OAA values with all testing nodes (h1: 10 – 40) and convenience to design the ANN networks, for identifying the 11 species, all ANNs use h1 = 25 or 30, η = 0.8 or 0.7, and α = 0.1 0r 0.2 while for identifying 5 oak species, all ANNs use h1 = 16 or 20, η = 0.8 or 0.7, α = 0.1 or 0.2.

For classifying both 11 species and a subset of 5 oak species, the first row of Table 3 shows classification results calculated from three sets of test samples by ANN. From the table, we can see that the classification accuracies (OAA) of averaging three

runs of test samples are around 88% and Kappa values of 0. 87 and 0.84, respectively. The species recognition accuracies produced by ANN are acceptable when considering the spectral similarity among most of the 11 species (Figure 2).

With exactly the same inputs of 30 selected spectral variables as for ANN for both 11 species and 5 oak species recognition, it is apparent that all accuracy indices produced by LDA are very close to those by ANN, including both OAA and Kappa values. The recognition accuracies generated by ANN and LDA are not statistically different (Z<0.24), indicating, for this particular case, that a non-linear recognition method does not outperform a linear method. It might be due to most selected spectral variables following a normal distribution by their corresponding spectral samples.

Algorithm	Overall accuracy (%)		Kappa value	
	11species	5 oak species	11 species	5 oak species
ANN	87.82	87.49	0.8656	0.8428
LDA	86.80	86.31	0.8546	0.8280

Note: The overall accuracies produced by ANN and LDA are not significantly different at 0.95 confidence level for identifying either 11 species or 5 oak species

Table 3. Summary of species identification accuracy using ANN and LDA algorithms with 30 selected spectral variables.

5. DISCUSSION

In this analysis, among the 30 selected spectral variables evaluated by ANOVA, most of the spectral variables are directly related to leaf chemistry, especially water status and chlorophyll content in leaves. For example, some selected spectral variables relate to water absorption bands: WI, DEP-975, AREA-975, and Ratio975 directly relate to the 970 nm water absorption band; Ratio1200, NDWI, E-1D, DEP-1200, AREA-1200, and WID-1200 are directly correlated with the 1200 water absorption band; and DSWI relates to the 1750 water absorption band. Other spectral variables relate to chlorophyll content: C-1D, A-1D, B-1D, R550, A-WP, LCI, B-WP, NDVI, SR, C-WP, and R680 that may directly describe the variation of leaf chlorophyll content. In general, the full range (350 nm to 2500 nm) of spectral wavelength covered by the ASD spectrometer is useful for differentiating species that differ in their foliage content, water status, pigment content and other biochemicals, including visible, near infrared (NIR) and middle infrared (MIR) regions (Nagendra, 2001). However, due to the heavy water absorption bands near 1.4 μm and 1.9 μm, which always happen in *in situ* spectral measurement, visible and NIR bands are generally more useful than MIR bands. In this case, most of the spectral variables with high frequency of spectral separabilty between any paired-species have been constructed from some of the visible and NIR bands.

Although the recognition accuracy (around 88%) derived from this study is acceptable for *in situ* species differentiation much work is needed before applying this method to remote-sensing image data, including high spatial resolution data, e.g., IKONOS (Carleer and Wolff, 2004) and QuickBird (Wang et al., 2004) or hyperspectral data, e.g., AVIRIS (Xiao et a., 2004) and HyMap (Buddenbaum et al., 2005). In this study, atmospheric effects on the *in situ* hyperspectral measurements was minimal except for the two major water absorption bands in the MIR region. However, for remote-sensing image data, atmospheric effects have to be corrected or compressed before conducting a species recognition analysis (Nagendra, 2001;

Clark et al., 2005). Atmospheric correction will enhance the spectral separability between species with multi/hyperspectral remote-sensing data. Even so, the preliminary results with the *in situ* hyperspectral data imply that current remote-sensing techniques are still difficult but possible to identify similar species to such 11 broadleaf species with an acceptable accuracy.

6. CONCLUSIONS

The ANOVA analysis results indicate that the extracted 30 spectral variables are effective for differentiating the 11 species. The 30 selected spectral variables include spectral variables related to water absorption bands: WI, DEP-975, AREA-975, and Ratio975 (directly related to the 970 nm water absorption band); Ratio1200, NDWI, E-1D, DEP-1200, AREA-1200, and WID-1200 (directly correlated to the 1200 water absorption band); and DSWI (related to the 1750 water absorption band). The remaining spectral variables relate to chlorophyll content: C-1D, A-1D, B-1D, R550, A-WP, LCI, B-WP, NDVI, SR, C-WP, and R680 (may directly describe the variation of leaf chlorophyll content). Both classification algorithms (ANN and LDA) produced acceptable accuracies (OAA from 86.3 % to 87.8%, Kappa from 0.83 to 0.87). In this study, ANN and LDA for classifying the 11 broadleaf species have a similar performance and the difference of species recognition accuracies between the two classification algorithms is not statistically significant at 0.95 confidence level. The preliminary results of identifying the 11 species with the *in situ* hyperspectral data imply that current remote-sensing techniques, including high spatial and spectral sensors' data, are still difficult but possible to identify similar species to such 11 broadleaf species with an acceptable accuracy.

REFERENCES

Asner, G. P., Palace, M., Keller, M., Pereira, R., Silva, J. N. M., and Zweede, J. C., 2002. Estimating canopy structure in an Amazon Forest from laser range finder and IKONOS satellite observations. *Biotropica*, 34 (4), 483-492.

Barnes, J. D., Balaguer, L., Manrique, E., Elvira, S., and Davison., A. W., 1992. A reappraisal of the use of DMSO for the extraction and determination of chlorophylls a and b in lichens and higher plants. *Environ. Exp. Bot.*, 32, 85–100.

Biging, G. S., Congalton, R. G., and Murphy, E. C., 1991. A comparison of photointerpretation and ground measurements of forest structure. In Proceedings of the 57th Annual Meeting of American Society for Photogrammetry and Remote Sensing, March, 1991, Baltimore,Md., 6-15.

Brockhaus, J. A., and Khorram, S., 1992. A comparison of SPOT and Landsat TM data for use in conducting inventories of forest resources, International Journal of Remote Sensing, 13: 3035-3043.

Buddenbaum, H., Schlerf, M., and Hill, J., 2005. Classification of coniferous tree species and age classes using hyperspectral data and geostatistical methods. *International Journal of Remote Sensing*, 26(24), 5453-5465.

Campbell, K. and Landry, S., 1999. *City of Tampa Urban Ecological Analysis,* The Florida center for Community design and Research, University of South Florida.

Carleer, A. and Wolff, E., 2004. Exploition of very high resolution satellite data for tree species identification, *Photogrammetric Engineering and Remote Sensing*, 70(1), 135-140.

Carreiras, J. M. B., Pereira, J. M. C., and Pereira, J. S., 2006. Estimation of tree canopy cover in evergreen oak woodlands using remote sensing. Forest Ecology and Management, 223 (1-3), 45-53.

Clark, M. L., Roberts, D. A., and Clark, D. B., 2005. Hyperspectral discrimination of tropical rain forest tree species at leaf to crown scales. *Remote Sensing of Environment*, 96, 375-398.

Cochrane, M. A., 2000. Using vegetation reflectance variability for species level classification of hyperspectral data. *International Journal of Remote Sensing*, 21(10), 2075-2087.

Congalton, R., Miguel-Ayanz, J., and Gallup, B., 1991. Remote sensing techniques for hardwood mapping. Contract Rep. to California Dept. of Forestry and Fire Protection, Sacramento, California.

Datt, B., 1999. A new reflectance index for remote sensing of chlorophyll content in higher plants: tests using Eucalyptus leaves. *J. Plant Physiol.*, 154, 30-36.

Datt, B., McVicar, T.R., Van Niel, T.G., Jupp, D.L.B., and Pearlman, J.S., 2003. Preprocessing EO-1 Hyperion hyperpsectral data to support the application of agricultural indexes. IEEE Trans. Geosci. Remote Sens., Vol. 41, pp. 1246-1259.

Franklin, S. E., 1994. Discrimination of subalpine forest species and canopy density using digital CASI, SPOT, and Landsat TM data. *Photogrammetric Engineering and Remote Sensing*, 60, 1233-1241.

Galvão, L. S., Formaggio, A. R., and Tisot, D. A., 2005. Discrimination of sugarcane varieties in Southeastern Brazil with EO-1 Hyperion data. *Remote Sensing of Environment*, 94, 523-534.

Gao, B.C., 1996. NDWI – A normalized difference water index for remote sensing of vegetation liquid water from space. *Remote Sensing of Environment*, 58, 257-266.

Gong, P. and Chen, J., 1992. Boundary uncertainties in digitized maps I: some possible determination methods. In *Proceedings of the 1992 Geographic Information System & Land Information System*, November, 1992, San Jose, California, 274-281.

Gong, P., Biging, G. S., Lee, S. M., Mei, X., Sheng, Y., Pu, R., Xu, B., Schwarz, K. P., and Mostafa, M., 1999. Photo ecometrics for forest inventory. *Geographic Information Sciences*, 5(1), 9-14.

Gong, P., Pu, R. and Yu, B., 1997. Conifer species recognition: An exploratory analysis of in situ hyperspectral data. *Remote Sensing of Environment*, 62, 189-200.

Gong, P., Pu, R., and Heald, R. C., 2002. Analysis of in situ hyperspectral data for nutrient estimation of giant sequoia. *International Journal of Remote Sensing*, 23(9), 1827-1850.

Johansen, K. and Phinn, S., 2006. Mapping structural parameters and species composition of riparian vegetation using IKONOS and Landsat ETM plus data in Australian tropical savannahs. *Photogrammetric Engineering and Remote Sensing*, 72 (1), 71-80.

Jordan, C. F., 1969. Derivation of leaf area index from quality of light on the forest floor. Ecology, 50, 663-666.

Nagendra, H., 2001. Using remote sensing to assess biodiversity. *International Journal of Remote Sensing*, 22(12), 2377-2400.

Peñuelas, J., and Filella, I., 1998. Visible and near-infrared reflectance techniques for diagnosing plant physiological status. *Trends in Plant Science*, 3, 151–156.

Peñuelas, J., Filella, I., Lloret, P., Muñoz, F., and Vilajeliu, M., 1995. Reflectance assessment of mite effects on apple trees. *Int. J. Remote Sens,* 16, 2727–2733.

Peñuelas, J., Gamon, J.A., Fredeen, A.L., Merino, J., and Field, C.B., 1994. Refelctance indices associated with physiological changes in nitrogen- and water-limited sunflower leaves. *Remote Sens. Environ.,* 48, 135–146.

Peñuelas, J., Piñol, J., Ogaya, R., and Filella, I., 1997. Estimation of plant water concentration by the reflectance water index WI (R900/R970). *Int. J. Remote Sens.*, 18, 2869-2875.

Pu, R., Foschi, L., and Gong, P., 2004. Spectral feature analysis for assessment of water status and health level of coast live oak (Quercus Agrifolia) leaves. *International Journal of Remote Sensing*, 25(20), 4267-4286.

Pu, R., Ge, S., Kelly, N.M., and Gong, P., 2003. Spectral absorption features as indicators of water status in Quercus Agrifolia leaves. *International Journal of Remote Sensing*, 24(9), 1799-1810.

Rouse, J. W., Haas, R. H., Schell, J. A., and Deering, D. W., 1973. Monitoring vegetation systems in the Great Plains with ERTS," in *Proceedings, Third ERTS Symposium, vol. 1*, pp. 48-62, 1973.

SAS Institute Inc., 1991. *SAS/STA User's Guide*, Release 6.03 Edition, Gary, NC: SAS Institute Inc., USA, 1028pp.

Thenot, F., Méthy, M., and Winkel, T. (2002). The Photochemical reflectance index (PRI) as a water-stress index. *Int. J. Remote Sens.*, 23, 5135-5139.

Thomas, J.R., and Gausman. H.W., 1977. Leaf reflectance vs. leaf chlorophyll and carotenoid concentration for eight crops. *Agron. J.* 69, 799–802.

Tian, Q., Tong, Q., Pu, R., Guo, X., and Zhao, C., 2001. Spectroscopic determination of wheat water status using 1650-1850 nm spectral absorption features. *International Journal of Remote Sensing*, 22(12), 2329-2338.

Wang, L., Sousa, W. P., Gong, P., and Biging, G. S., 2004. Comparison of IKONOS and QuickBird images for mapping mangrove species on the Caribbean coast of Panama. *Engineering and Remote Sensing*, 91(3-4), 432-440.

Xiao, Q., Ustin, S. L., and McPherson, E. G., 2004. Using AVIRIS data and multiple-masking techniques to map urban forest tree species. *International Journal of Remote Sensing*, 25(24), 5637-5654.